

Grouped Mixture of Regressions

Haidar Almohri[†], PhD

Ratna Babu Chinnam[†], Ph.D., Professor

Arash A. Amini[‡], Ph.D, Professor *

[†]Department of Industrial and Systems Engineering
Wayne State University, Detroit, MI 48201, U.S.A.

[‡]Department of Statistics

University of California, Los Angeles

{*Haidar.Almohri, Ratna.Chinnam*}@wayne.edu

AAAmini@ucla.edu

March 27, 2022

Abstract

Finite Mixture of Regressions (FMR) models are among the most widely used approaches for dealing with heterogeneity in regression problems. One of the limitations of current FMR approaches is their inability to incorporate group structure in data when available. In some applications, it is desired to cluster groups of observations together rather than the individual ones. In this work, we extend the FMR framework to allow for group structure among observations, and call the resulting model the Grouped Mixture of Regressions (GMR). We offer a fast algorithm for estimating the model parameters using Expectation-Maximization (EM). We also show how the group structure can improve prediction by sharing information among members of each group, as reflected in the posterior predictive density under GMR. The performance of the approach is assessed using both synthetic data as well as a real-world example.

Keywords: data heterogeneity; grouped data; mixture models; mixture models with must-link constraint; predictive modeling.

*The authors gratefully acknowledge the support of *Urban Science* for sponsoring this research.

1 Introduction

One of the challenges in modeling certain populations is that the observations might be drawn from different underlying processes. In such cases, a “single” model may fail to efficiently represent the entire sample and as a result the accuracy and reliability of the model would suffer. This problem has been identified more than a hundred years ago ([Newcomb, 1886](#); [Pearson, 1894](#)) and “mixture models” were introduced in order to better account for the unobserved heterogeneity in the population. Since those early days, a lot of effort has gone into developing new methodologies and improving the existing models. In recent years, due to increasing availability and diversity of data, the topic has gained renewed interest among the researchers. Mixture models are being successfully employed in a variety of diverse applications such as speech recognition ([Reynolds et al., 1995](#)), image retrieval ([Permuter et al., 2003](#)), term structure modeling ([Lemke, 2006](#)), biometric verification ([Stylianou et al., 2005](#)), and market segmentation ([Tuma and Decker, 2013](#)).

Among the family of mixture models, Finite Mixture of Regressions (FMR) models have been particularly popular in various fields and applications ([Bierbrauer et al., 2004](#); [Andrews and Currim, 2003](#); [Bar-Shalom, 1978](#)). This is mainly due to advantages of linear models such as simplicity, interpretability, and scientific acceptance. In FMR, it is assumed that the distribution of data can be represented using a convex combination of a finite (K) number of linear regression models. Equivalently, each observation belongs to one of the K classes, and given a class membership, it follows the regression model associated with that class. The difficulty is that the class memberships are not known in advance.

Estimating the Parameters. FMR parameter estimation has been studied mainly from a likelihood point of view ([De Veaux, 1989](#)), with exceptions such as [Quandt and Ramsey \(1978\)](#) where moment generating functions are used. The maximum likelihood approach using Expectation Maximization (EM) ([Dempster et al., 1977](#)) remains the most widely used technique for estimating the parameters of the FMR. EM is an iterative procedure that is guaranteed to increase the likelihood at each step. As a by-product, one obtains approximate posterior distributions of the latent class memberships as well. Other algorithms such as stochastic EM ([Celeux and Diebolt, 1985](#)) and classification EM ([Celeux](#)

and Govaert, 1992) have also been introduced as an attempt to improve the performance of the EM algorithm; see Faria and Soromenho (2010) for good discussion.

1.1 FMR with Group Structure

Under the regular FMR setting, the response variable follows a mixture model where each component is a linear regression model based on the underlying covariates. In addition to the parameters of the regression models, FMR assigns a class membership to each observation along with a prior probability of belonging to each component. The result is equivalent to soft clustering of the observations into K clusters, assuming K components are employed. In some applications however, instead of individual observations, groups of observations are to be clustered or associated with the same component. For example, if the FMR is being employed to model data from a retail chain, it might be necessary to associate all observations stemming from any single store to the same component.

This problem is similar to what is known as “clustering with must-link constraint”, which was introduced by Wagstaff et al. (2001). The main idea is to utilize experts’ domain knowledge prior to clustering process in order to obtain desired properties from the clustering solution. Figure 1.1 illustrates the concept. The data points are synthetically generated using two components: $y_1 = \frac{1}{2}x + \epsilon_1$ and $y_2 = \frac{3}{4}x + \epsilon_2$, where $x \sim \mathcal{N}(0, 1)$, $\epsilon_1 \sim \mathcal{N}(0, 0.5)$, and $\epsilon_2 \sim \mathcal{N}(0, 0.3)$. Figure 1a shows the linear relationship between the two groups (y_1 and y_2), without any grouping (must-link) structure. In Figure 1b, the data points are linked to create six groups (groups 1-3 belong to model y_1 and groups 4-6 to y_2). Data points with the same color belong to the same group. The desired outcome is to have all the data points in the same group end up having the same class membership. See Basu (2009) for a good discussion of constrained clustering algorithms and applications.

Almohri et al. (2018) proposed a non-parametric, heuristic solution to the grouping problem called Mixture Models with Competitive Learning (MMCL). They developed an iterative algorithm that given the current estimated component regression models, assigns each group to the cluster that best predicts the observations of that group in terms of the employed loss function. The component regression models are then updated by fitting a regression model to the aggregated observations assigned to each cluster. The procedure

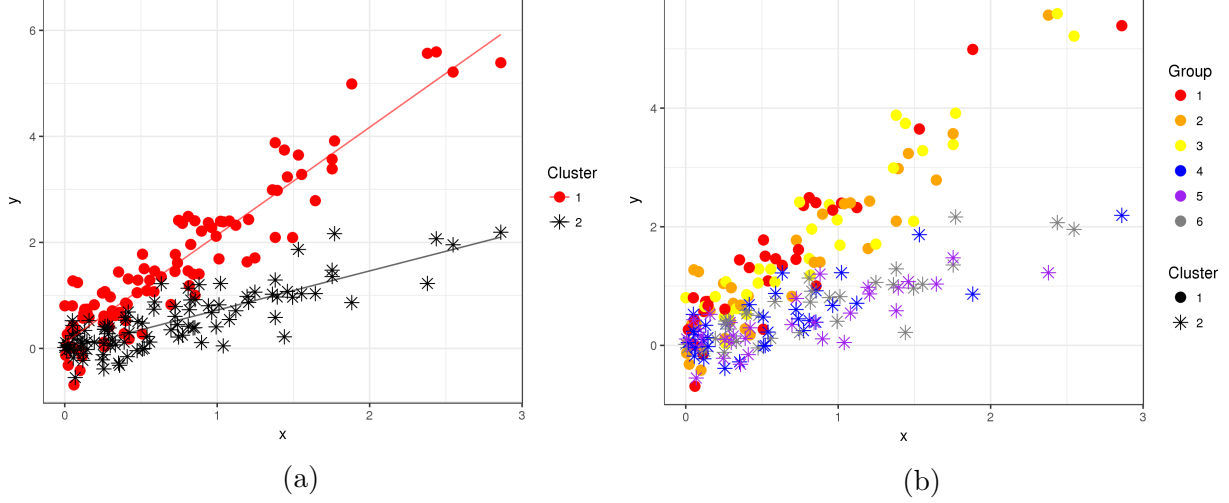


Figure 1: FMR with “group” constraint: (a) Synthetic, two-component FMR without any constraint. (b) The same data divided into six groups where each group has to retain its data points.

bears resemblance to the k -means clustering technique, with Euclidean distance replaced with prediction loss for the group. [Almohri et al. \(2018\)](#) also provide an extension to MMCL, called MMCL++, that helps select the initial groups.

To the best of our knowledge, the work of [Almohri et al. \(2018\)](#) is the only attempt that addresses FMR with group structure in the literature. In contrast to their heuristic approach, we provide an exact parametric solution to this problem. We also derive an iterative likelihood-based parameter estimation algorithm for the model based on EM.

1.2 Grouped Mixture of Regressions (GMR)

We assume that the observations belong to R *known groups*, denoted with labels $[R] := \{1, \dots, R\}$. In each group $r \in [R]$, we observe n_r samples $(y_{ri}, x_{ri}), i = 1, \dots, n_r$ where $y_{ri} \in \mathbb{R}$ is the response variable and $x_{ri} \in \mathbb{R}^p$ is the vector of covariates or features. We will write x_{rij} to denote the j^{th} feature in the feature vector x_{ri} . For the most part, we will treat x_{ri} as deterministic observations, i.e., we have *fixed design* regression models.

We assume that there are K latent (unobserved) clusters (data generating processes) and that all the observations in any group r belong to a single cluster. Thus, we can assign a cluster membership variable $z_r \in \{0, 1\}^K$ to each group $r \in [R]$. We will have $z_{rk} = 1$ iff group r belongs to cluster k . With some abuse of notation, we also write $z_r = k$ in place

of $z_{rk} = 1$. Given the cluster membership variable z_r , we assume that group r observations are independent draws from a Gaussian linear regression model with parameters specified by z_r , that is,

$$p(y_{ri} | z_r = k) \stackrel{\text{indep}}{\sim} \mathcal{N}(\beta_k^T x_{ri}, \sigma_k^2), \quad i = 1, \dots, n_r, \quad (1)$$

where $\beta_k \in \mathbb{R}^p$ is the coefficient vector of the k th regression model and σ_k^2 is the noise variance for component k . Note that we are assuming that the noise level only depends on the underlying cluster and not on the group. We write $\beta = (\beta_1 | \dots | \beta_K) \in \mathbb{R}^{p \times K}$ and $\sigma^2 = (\sigma_1^2, \dots, \sigma_K^2) \in \mathbb{R}^K$.

As is common in mixture modeling, we assume that z_r follows a multinomial prior with parameter $\pi = (\pi_k)$, that is, $\mathbb{P}(z_r = k) = \pi_k$ for $k \in [K]$, and z_1, \dots, z_R are drawn independently. The joint distribution of y_r and z_r is then given by:

$$p_\theta(y_r, z_r) = p_\theta(z_r) \prod_{i=1}^{n_r} p_\theta(y_{ri} | z_r) = \prod_{k=1}^K \left[\pi_k \prod_{i=1}^{n_r} p_\theta(y_{ri} | z_r = k) \right]^{z_{rk}} \quad (2)$$

where we let $\theta = (\beta, \pi, \sigma^2)$ denote the collection of all the model parameters. From (1), we have $p_\theta(y_{ri} | z_r = k) = \phi_{\sigma_k}(y_{ri} - \beta_k^T x_{ri})$, where $\phi_\sigma(\cdot)$ is the density of the Gaussian distribution $\mathcal{N}(0, \sigma^2)$. Therefore, the complete likelihood of θ given (z, y) is:

$$L(\theta | y, z) = p_\theta(y, z) = \prod_{r=1}^R p_\theta(y_r, z_r) = \prod_{r=1}^R \prod_{k=1}^K \underbrace{\left[\pi_k \prod_{i=1}^{n_r} \phi_{\sigma_k}(y_{ri} - \beta_k^T x_{ri}) \right]^{z_{rk}}}_{=: \gamma_{rk}(\theta)} \quad (3)$$

The parameter $\gamma_{rk}(\theta)$ in (3) is proportional (in k) to the posterior probability of z_r given the observation y_r , that is, $p_\theta(z_r = k | y_r) \propto_k p_\theta(y_r, z_r = k) = \gamma_{rk}(\theta)$. By normalizing $\gamma_{rk}(\theta)$ over k , we obtain the *posterior probability of cluster assignments*:

$$p_\theta(z_r = k | y_r) = \frac{\gamma_{rk}(\theta)}{\sum_{k'} \gamma_{rk'}(\theta)} =: \tau_{rk}(\theta), \quad (4)$$

for any $k \in [K]$ and $r \in [R]$. We note that the overall posterior factorizes over groups, i.e., $p_\theta(z | y) = \prod_r p_\theta(z_r | y_r)$, so it is enough to specify it for each pair of z_r and y_r . Thus, $\tau_{rk}(\theta)$

is the posterior probability that group r belongs to cluster k , given all the observations y . These posterior probabilities are key estimation objectives.

An estimate $\hat{\theta} = (\hat{\beta}, \hat{\phi}, \hat{\sigma}^2)$ of θ can be obtained by maximizing (3). The classical approach to performing such optimization is by the Expectation Maximization (EM) algorithm, the details of which will be given in Section 1.4. Once we have an estimate $\hat{\theta}$ of the parameters, we can calculate an estimate of the posterior probabilities as $\tau_{rk}(\hat{\theta})$.

1.3 Posterior Prediction with GMR

Now assume that we have a new test data point $(y_{r,\text{new}}, x_{r,\text{new}})$ in group r , for which we observe only the feature vector $x_{r,\text{new}}$ and would like to predict $y_{r,\text{new}}$. Let $(y^{\text{train}}, x^{\text{train}})$ denote all the observations used in the training phase. The common link between the training and test data points are the latent variables z_1, \dots, z_R . In other words, since we already have a good estimate of the membership of group r based on the training data (via the posterior (4)), we can obtain a much better prediction of $y_{r,\text{new}}$ than what the prior model suggests. More precisely, the *predictive density* for $y_{r,\text{new}}$ based on y^{train} is:

$$p_{\theta}(y_{r,\text{new}} | y^{\text{train}}) = \sum_{z_r} p_{\theta}(y_{r,\text{new}} | z_r) p_{\theta}(z_r | y^{\text{train}}).$$

Since, $p_{\theta}(z_r = k | y^{\text{train}}) = p_{\theta}(z_r = k | y_r^{\text{train}}) = \tau_{rk}(\theta)$, we obtain the following estimate of the predictive density:

$$\begin{aligned} p_{\hat{\theta}}(y_{r,\text{new}} | y^{\text{train}}) &= \sum_{k=1}^K p_{\theta}(y_{r,\text{new}} | z_r = k) \tau_{rk}(\hat{\theta}) \\ &= \sum_{k=1}^K \tau_{rk}(\hat{\theta}) \phi_{\hat{\sigma}_k}(y_{r,\text{new}} - \hat{\beta}_k^T x_{r,\text{new}}). \end{aligned} \tag{5}$$

Note that $\hat{\theta}$ is our estimate of the parameters based on the training data $(y^{\text{train}}, x^{\text{train}})$. In particular, the posterior mean based on (5) is $\sum_{k=1}^K \tau_{rk}(\hat{\theta}) \hat{\beta}_k^T x_{r,\text{new}}$, which serves as the maximum a posteriori (MAP) prediction for $y_{r,\text{new}}$.

To summarize, since the membership group of the new observation is known, we obtain a predictive density of the form (5) for new observations. Thus, we can utilize the group

structure to leverage the information acquired during training phase when predicting new observations. This allows us to achieve a better prediction accuracy using the (posterior) latent cluster assignment. This type of information sharing between the training and test data does not occur in the usual FMR and is a unique strength of the proposed GMR model. In the usual FMR, the posterior mean predicted for a new data point will be the prior average of the mixture components: $\sum_{k=1}^K \pi_k \hat{\beta}_k^T x_{\text{new}}$, and the only sharing that occurs between the training and test data is via the estimated parameters $\{\hat{\beta}_k\}$.

1.4 GMR Parameter Estimation

Let us now derive the EM updates for the model. Recalling (3), the complete log-likelihood of the model is $\ell(\theta | y, z) = \log p_\theta(y, z) = \sum_{r=1}^R \sum_{k=1}^K z_{rk} \log \gamma_{rk}(\theta)$, or

$$\ell(\theta | y, z) = \log p_\theta(y, z) = \sum_{r=1}^R \sum_{k=1}^K z_{rk} \left[\log \pi_k + \sum_{i=1}^{n_r} \log \phi_{\sigma_k}(y_{ri} - \beta_k^T x_{ri}) \right]. \quad (6)$$

Treating the class latent memberships $\{z_r\}$ as missing data, we perform the EM updates to simultaneously estimate $\{z_r\}$ and θ :

E-Step: Replace (6) with its expectation under the approximate posterior of $\{z_r\}$:

$$F(\theta; \hat{\theta}) := E_{z \sim \tau(\hat{\theta})}[\ell(\theta | y, z)] = \sum_{r=1}^R \sum_{k=1}^K \tau_{rk}(\hat{\theta}) \log \gamma_{rk}(\theta) \quad (7)$$

using $\mathbb{E}_{z \sim \tau(\hat{\theta})}[z_{rk}] = \tau_{rk}(\hat{\theta})$, where $\tau_{rk}(\theta)$ is the posterior given in (4).

M-Step: Maximize $F(\theta; \hat{\theta})$ over θ , giving the update rules for the parameters $\theta = (\beta, \pi, \sigma^2)$.

To derive the update rules, we maximize $F(\theta; \hat{\theta})$ by a sequential block coordinate ascent approach, in each step maximizing over one of the three sets of parameters π, β and σ^2 , while fixing the others. The updates are summarized in Algorithm 1. The details can be found in Appendix A.

Algorithm 1 Grouped mixture of regressions (GMR)

- 1: Compute feature covariances for each group: $\hat{\Sigma}_r \leftarrow \frac{1}{n_r} \sum_{i=1}^{n_r} x_{ri} x_{ri}^T$
- 2: Compute feature-response cross-covariances: $\hat{\rho}_r \leftarrow \frac{1}{n_r} \sum_{i=1}^{n_r} y_{ri} x_{ri}$
- 3: For any class posterior $\tau = (\tau_{rk})$ define the following weights:

$$\tau_{+k}(\tau) := \sum_r \tau_{rk}, \quad w_{rk}(\tau) := n_r \tau_{rk}, \quad w_{+k}(\tau) := \sum_r w_{rk}, \quad \check{w}_{rk}(\tau) := \frac{w_{rk}}{w_{+k}}.$$

and the weighted covariances: $\tilde{\Sigma}_k(\tau) := \sum_{r=1}^R \check{w}_{rk} \hat{\Sigma}_r$ and $\tilde{\rho}_k(\tau) := \sum_{r=1}^R \check{w}_{rk} \hat{\rho}_r$.

- 4: For any parameter $\theta = (\pi, \beta, \sigma^2)$ and class posterior $\tau = (\tau_{rk})$, define the errors:

$$E_{rk}(\beta) := \frac{1}{n_r} \sum_i^{n_r} (y_{ri} - \beta_k^T x_{ri})^2, \quad \bar{E}_k(\beta, \tau) := \sum_r \check{w}_{rk}(\tau) E_{rk}(\beta)$$

- 5: **while** not converged **do**

- 6: Update class frequencies: $\pi_k \leftarrow \tau_{+k}(\tau)/R, \quad k \in [K]$
- 7: Update regression coefficients: $\beta_k \leftarrow \tilde{\Sigma}_k^{-1}(\tau) \tilde{\rho}_k(\tau), \quad k \in [K]$
- 8: Update noise variances: $\sigma_k^2 \leftarrow \bar{E}_k(\beta, \tau), \quad k \in [K]$
- 9: Update class memberships: $\tau_{rk} \leftarrow \tau_{rk}(\theta)$, as given in (4), $r \in [R], k \in [K]$

- 10: **end while**
-

2 Empirical Analysis

A Monte Carlo simulation study was performed to assess the quality of the proposed GMR algorithm. The results of this study is presented in this section.

Experiment setup. We generate the synthetic data from the GMR model (1) with a random design where the feature vectors are drawn as $x_i \sim N(0, \Sigma)$ given Σ . The covariance matrix Σ is itself drawn from a normalized Wishart distribution. Recall that K is the number of clusters (or mixture components) and R the number of groups. In most of the experiments, we use equal number of observations per group, that is, n_r is the same for all $r = 1, \dots, R$. Letting $n = \sum_{r=1}^R n_r$ be the total number of observations, we have $n_r = n/R$. Let G_k be the number of groups in cluster k . In general, $\sum_{k=1}^K G_k = R$; here, we take all G_k to be equal so that $G_k = G := R/K$. Thus, it is enough to specify n, G , and K . Table 1 summarizes various setups used in our simulations. We recall that p is the dimension of the feature vectors x_i and “the noise level” is σ_k in (1). In each case, the

Table 1: Monte Carlo Simulation Parameters

K	p	G	n	Noise Level (σ_k)	β -distance (δ_β)
2	2	10	(100, 200, 400, 800)	(2, 4, 6, 8, 10)	(4, 8, 12)
4	(2, 4)				

number of groups R and the number of observations per group n_r is determined by the number of clusters K , number of groups in each cluster G , and total number of observations n . For example, for $n = 800$, $G = 10$, and $K = 2$, we have $R = 20$ and $n_r = 40$.

To study the effect of heterogeneity among regression coefficient vectors $\beta_k, k \in [K]$, we take β_k s to be equidistant points on a hypersphere in \mathbb{R}^p and vary their common distance, which we term β -distance and denote as δ_β . More precisely, we will have $\|\beta_k\| = \|\beta_\ell\|$ and $\|\beta_k - \beta_\ell\| = \delta_\beta$ for all $k \neq \ell$. Generating β s this way enables us to effectively compare the estimation errors among different runs of the experiment. The comparison can be carried out across different setups by normalizing the calculated error by δ_β . Three values of δ_β that are found to be adequate for our experiments are also listed in Table 1. Obviously, the smaller the distance (the smaller the β s) the harder the cluster separation.

The above equidistant setup is designed so that the data points are not easily separable in the input or output spaces, i.e. solely based on the X or y values. The degree of separation is only controlled by β -distance (δ_β) while the noise level (σ_k) controls the uncertainty in relation between X and y . Figure 2 shows samples of the generated data for different scenarios. Note from the Figure that the clusters are not identifiable in X or y domains, whereas plotting y against X reveals the two clusters.

Evaluation criteria. The Monte Carlo simulations are repeated 250 times for each pair of β -distance and the noise level as well as pairs of p and K . This setup is maintained in all the experiments that will be discussed later in the manuscript. Four criterion are used to benchmark the performance of the algorithm: (1) Normalized mutual information (NMI) for assessing the clustering accuracy, (2) average β estimation error, (3) root mean squared error (RMSE) of prediction to assess the prediction power of the models, and (4) the number of iterations to study the rate of convergence and the speed of the algorithms.

NMI is a widely used measure for evaluating the quality of clustering algorithms when the true labels are available. Advantages of using NMI is its invariance to cluster label

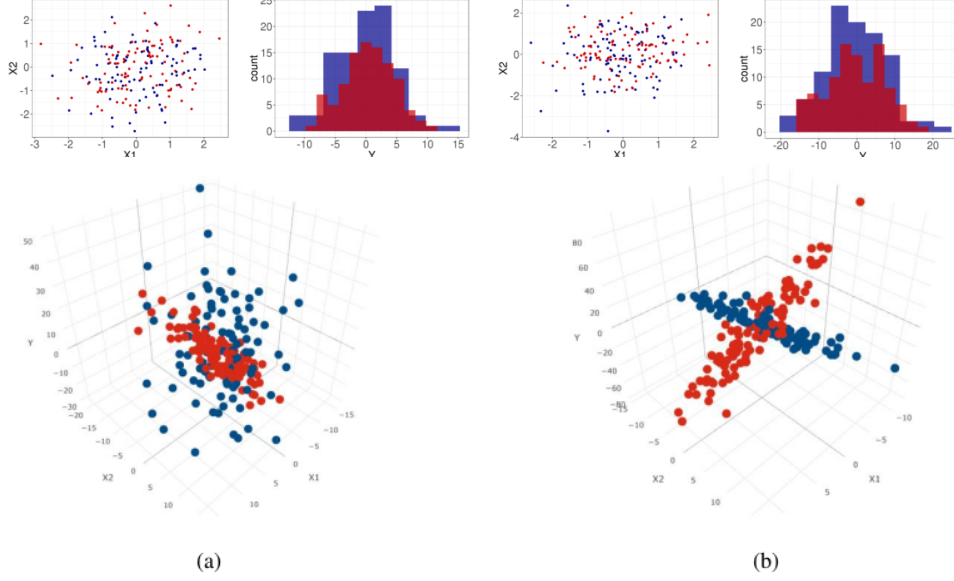


Figure 2: Sample of the generated data for simulation for the case $p = k = 2$: Covariates X (top left); the response values y (top right); 3d plot for the X and y (bottom): (a) $\delta_\beta = 4$, (b) $\delta_\beta = 12$

switching, and the aggressive penalization of the partitions close to random (relative to the true one). NMI is bounded between zero and one. The closer the value to zero, the higher the indication that the cluster assignments are largely independent, while a NMI close to one shows substantial agreement between the clusters.

“ β estimation error” is used as another measure of goodness of fit. We calculate this error by considering both the distance between the true and estimated β s, as well as the miss-classification error. More precisely, to each group r , we can assign two regression coefficient vectors, the estimated one $\hat{\beta}^{(r)}$, and the true one $\beta^{(r)}$; $\hat{\beta}^{(r)}$ is equal to $\hat{\beta}_k$ if we have estimated group r to be in cluster k . Similarly, $\beta^{(r)}$ is equal to β_k if group r is in true cluster k . We can define the average β estimation error as:

$$\text{avg err}_\beta := \frac{1}{R} \sum_{r=1}^R \|\hat{\beta}^{(r)} - \beta^{(r)}\|^2 = \text{tr}(D^T F) \quad (8)$$

where $D = (\|\hat{\beta}_k - \hat{\beta}_\ell\|^2, k, \ell \in [K])$ is the $K \times K$ matrix of pairwise squared distances between $\hat{\beta}_k$ s, and F is the confusion matrix between the estimated and true labels. The details for the second equality can be found in Appendix B.

Prediction RMSE is obtained by designating a hold-out (or test) set and using the

trained models to predict the responses over the hold-out set. In each simulation run, 80% of the observations in each group is used for training the model and 20% is held out to assess the prediction power. This setup is maintained in all the experiments that will be discussed later in the manuscript.

3 GMR Results

In this section we report in detail the results from the simulation and modeling experiments. Each factor of the study is presented in a subsection.

β -Distance (δ_β) and Noise Level (σ_k). Figure 3 is the result of running the experiments for the setup $n = 200$, $p = 4$, and $K = 4$. Referring to Figure 3, we observe that increasing σ_k (decreasing the signal to noise ratio) leads to a drop in the performance of the algorithm. This is also the case with δ_β , where we notice that the more separable the true β s are, the easier it is to estimate. We notice that at noise level $\sigma_k = 10$, and $\delta_\beta = 4$, NMI (Figure 3a) is close to zero, indicating that most of the times the algorithm fails to recover the true clusters. Similar trends are observed for the setup $n = 100$, $p = 2$, and $K = 2$, as illustrated by Figure 15 in Appendix C.

Dimensionality (p) and Number of Clusters (K). Figure 3 shows the NMI result for different combinations of p and K , with $n = 400$. Figure 4a and 4b, compare the result when K is fixed ($K = 2$) and the dimensionality is changed from $p = 2$ in 4a to $p = 4$ in 4b. Comparing the two plots, we can see slight improvement in the case where $p = 4$. To study the effect of increasing K , we can compare Figures 4b and 4c, where p is fixed ($p = 4$), and K is increased from $K = 2$ (Figure 4b) to $K = 4$ (Figure 4c). We can clearly see that the accuracy decreases in all cases (combinations of δ_β and σ_k). This is consistent with the fact that as the number of clusters (K) increases, it is always harder to recover true clusters. The results for β -estimation error are reported in Figure 16 in Appendix C.

Number of Groups in a Cluster. To study the impact of the number of observations per group, we set the total number of observations to $n = 100$ and take $K = 2$, which results

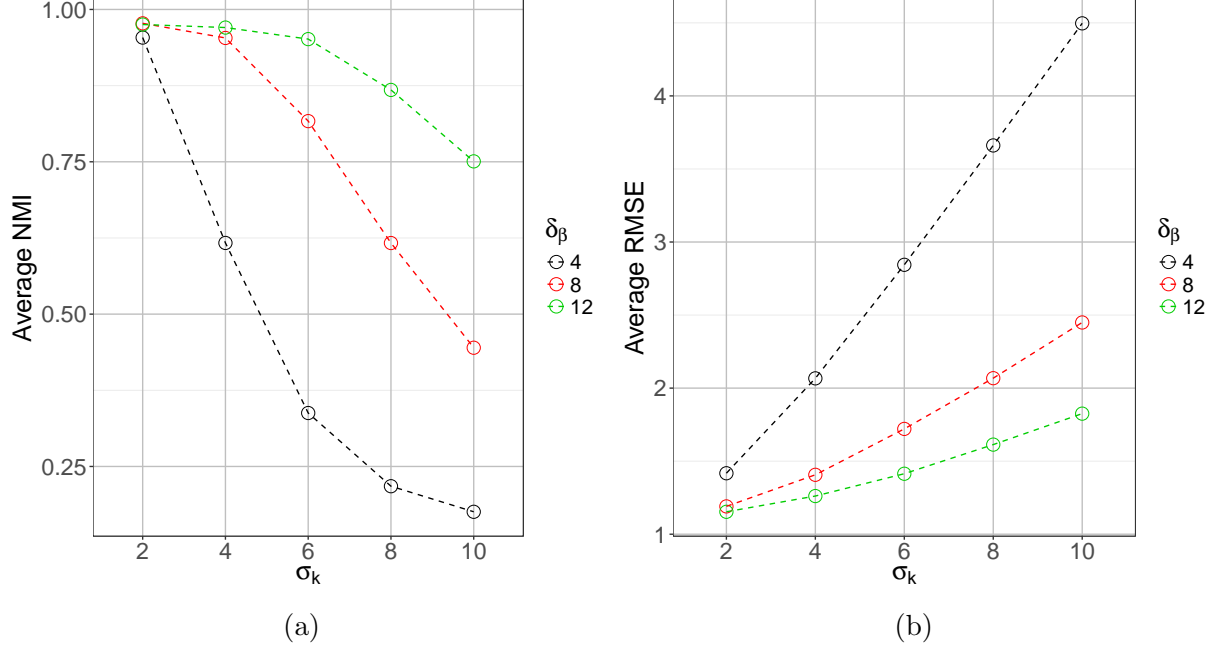


Figure 3: The effect of δ_β and σ_k for the case $n = 200, K = 4, p = 4$; each colored line in a plot represents different value of δ_β , x axis shows different values of σ_k , and y axis shows: (a) average NMI, (b) average RMSE for prediction.

in each cluster having 50 observations. We then vary the number of groups per cluster (G) from 50 down to 1 for each cluster, with $G = 50$ referring to the case where each observation is a single group, i.e., there is no grouping structure; whereas $G = 1$ is the case where all the observations in each cluster form a single group. In this setup, when varying G , we do not necessarily preserve equal number of observations per group (n_r), as in other experiments. If the observations can be equally distributed to all groups i.e. $G \in \{50, 25, 10, 5, 2, 1\}$, then there will be equal number of observations per group. In other cases, the observations are first equally distributed among the groups. The remaining observations are then assigned to the groups in a fashion that a group gets one extra observation until all the observations are distributed. For example, when $G = 48$, there will be 2 groups with 2 observations and 46 groups with single observations per cluster. Similarly, when $G = 16$, there will be 2 groups with 4 observations and 14 groups with 3 observations per cluster.

Figure 5 illustrates the result. We notice that as G increases, average NMI decreases, indicating the difficulty to recover the true class labels. This is expected because as we have more groups (G is larger), there are less observations in each group, which makes it

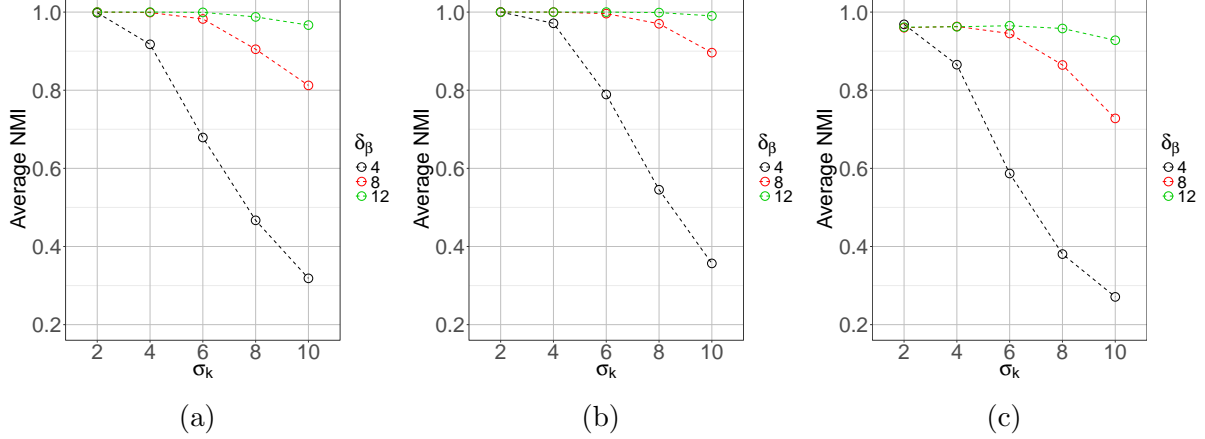


Figure 4: The impact of K and p on NMI for the case $n = 400$; each colored line in a plot represents different value of δ_β , x axis shows different values of σ_k , and y axis is average NMI for: (a) $K = 2, p = 2$, (b) $K = 2, p = 4$, (c) $K = 4, p = 4$.

difficult to utilize the grouping structure and therefore the performance drops.

Number of Iterations. One of the important factors in determining the effectiveness of an algorithm is its rate of convergence and its overall run time, which determines its suitability for high dimensional applications. Since the run time depends on several factors such as the platform, the quality of coding, hardware, etc. it is hard to report an accurate value for an algorithm. We report the average number of iterations for GMR convergence in each scenario as an estimated indicator for the speed of the algorithm.

The stopping rule is chosen to be the relative change in posterior probability of cluster assignments ($\tau_{rk}(\hat{\theta})$ in equation (4)). In particular, if we call $\tau_{rk}^{(t)}$ the posterior probabilities at iteration t , then the algorithm stops when $\|\tau^{(t-1)} - \tau^{(t)}\|_\infty < \epsilon$, where $\|\cdot\|_\infty$ is the infinity norm (maximum absolute row sum), or if the maximum number of iterations has been reached. In our setup, ϵ is set to 10^{-6} and the maximum number of iterations to 200. Figure 6 shows average number of iterations for selected scenarios. The y axis is shown in \log_2 scale to enhance visualization. Tables (2–5) in Appendix C provide full details of the results for the conducted simulation and modeling experiments mentioned in this section.

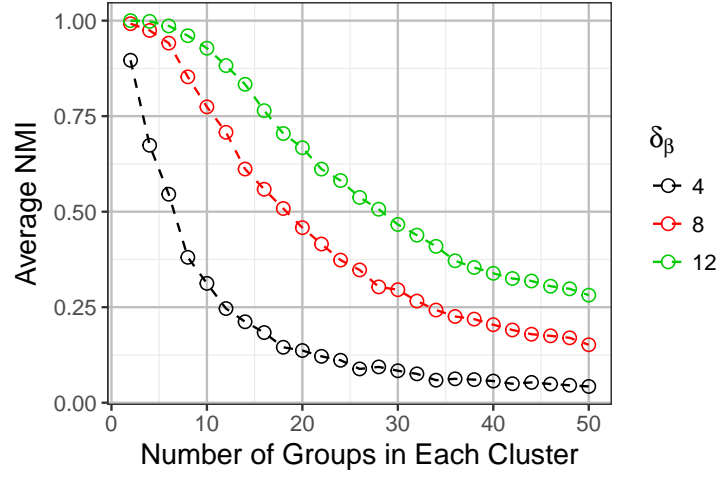


Figure 5: The effect of the number of groups per cluster (G) for the case $n = 100, K = 2$; each colored line in a plot represents a different value of δ_β ; x axis shows G which varies from 1 to 50 (only even numbers are plotted to enhance the quality). y axis shows the average NMI.

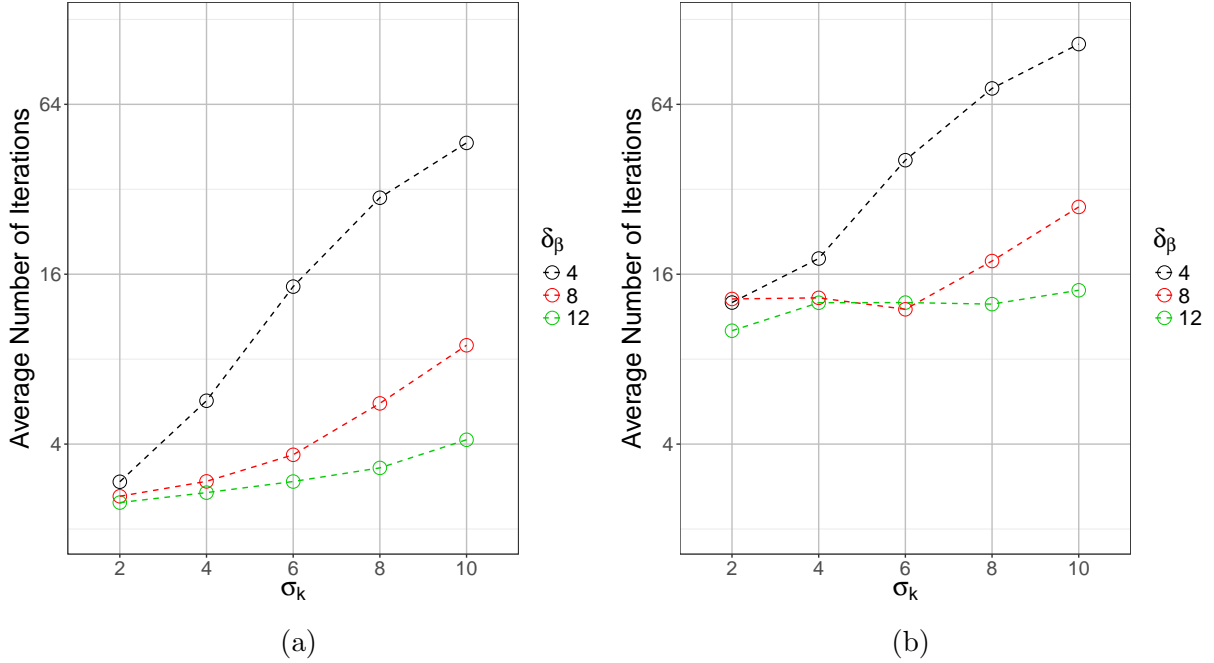


Figure 6: Average number of iterations for the case $n = 800$ (on \log_2 scale) for: (a) $K = 2, p = 2$, (b) $K = 4, p = 4$.

3.1 Selecting Optimal K

Selecting the number of components in a mixture model, which falls under the general problem of model selection, is a research topic that has attracted a lot of interest over years. Despite numerous advances, the problem is a fairly open question in statistics and machine learning, at least from a practical standpoint. Among the numerous methods introduced in the literature for determining the optimal number of clusters in a dataset, we refer to the following selective samples: [Goutte et al. \(1999\)](#), [Pelleg et al. \(2000\)](#), [Goutte et al. \(2001\)](#), [Lletí et al. \(2004\)](#) and [Honarkhah and Caers \(2010\)](#).

In the presence of independent variable(s), Cross-Validation (CV) is a simple and popular way of selecting the tuning parameters, including the best choice of K . To investigate the performance of CV under GMR in determining K , we set up an experiment with $\delta_\beta = (8, 12)$, $\sigma_k = 6$, and $N = 200$, where the data was generated using a true $K^* = 4$. GMR is trained on the data using $K = 2, \dots, 8$ clusters, and in each case the trained model is used to predict a held out set.

Figure 7 shows the plot of the average prediction RMSE against the K used in training. To compare the performance with some baselines, the test data is predicted using the mean (response y) of the training data as well as a single linear regression model. These two cases correspond respectively to $K = 0$ and $K = 1$ in Figure 7. One clearly observes that the GMR with $K > 1$ outperforms both the mean prediction ($K = 0$) and a single linear model ($K = 1$). The minimum error among the GMR models is attained with $K = 4$, which is the true number of components. The plot validates the ability of the algorithm to find the optimal number of components using CV.

3.2 Prediction Performance

As noted earlier in Section 1.3, the advantage of GMR over regular FMR is the posterior predictive density that enables us to utilize prior information about the group that a new observation is coming from. We claim that utilizing this prior knowledge can lead to a better prediction accuracy. To test the robustness of the prediction power of the model, we sample data by setting $n = 200$, $K = p = 4$, $\delta_\beta = 8$, $G = 10$ and train the GMR using the training data in each group. We then predict the hold-out set, first with

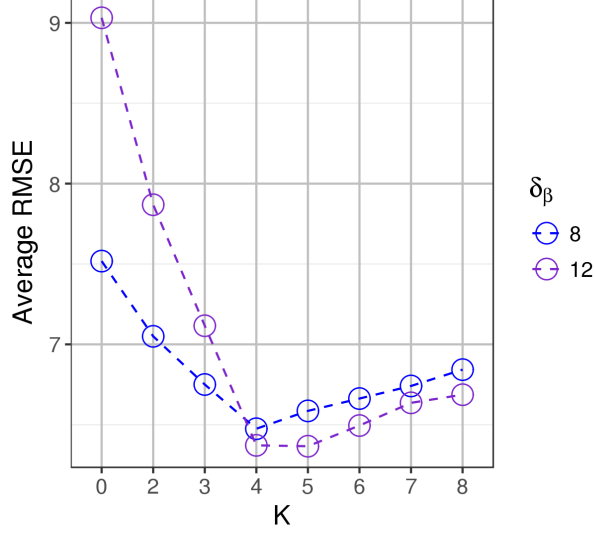


Figure 7: Finding the optimal value of K using cross validation: true $K^* = 4$. GMR is applied with different numbers of $K \in \{0, \dots, 8\}$ and they are shown in x axis in the graph. $K = 0$ refers to prediction by mean while $K = 1$ is the result of prediction using a single linear regression model.

the regular FMR and then with GMR. Note that in the case of regular FMR, once the model is trained and the parameters of the models are estimated, new observations will be predicted using the standard mixture model rule. In our group structure setup, we obtain the parameter estimates $\hat{\theta} = (\hat{\beta}_k, \hat{\sigma}_k, \pi_k; k \in \{1, \dots, K\})$ in the training phase. The MAP prediction using regular FMR is $y_{\text{new}} = \sum_{k=1}^K \pi_k \hat{\beta}_k^T x_{\text{new}}$ while that of the GMR is $y_{r,\text{new}} = \sum_{k=1}^K \tau_{rk}(\hat{\theta}) \phi_{\sigma_k}(y_{r,\text{new}} - \hat{\beta}_k^T x_{r,\text{new}})$ as discussed in Section 1.3. Figure 8 shows the resulting average RMSEs versus σ_k . It is clear that GMR prediction outperforms that of FMR indicating the improvement brought about by incorporating group membership information.

3.3 Comparing GMR with MMCL++

To perform a comparison between GMR and the existing method MMCL++ (Almohri et al., 2018), we ran both algorithms on the same data generated according to Table 1. Figure 9 illustrates the comparison of their ability for label recovery for the case $n = 100$ and $G = 10$. We can see that GMR outperforms MMCL++ in all cases in terms of correctly recovering the true labels. Figure 10 compares the prediction power of the two algorithms in terms of the

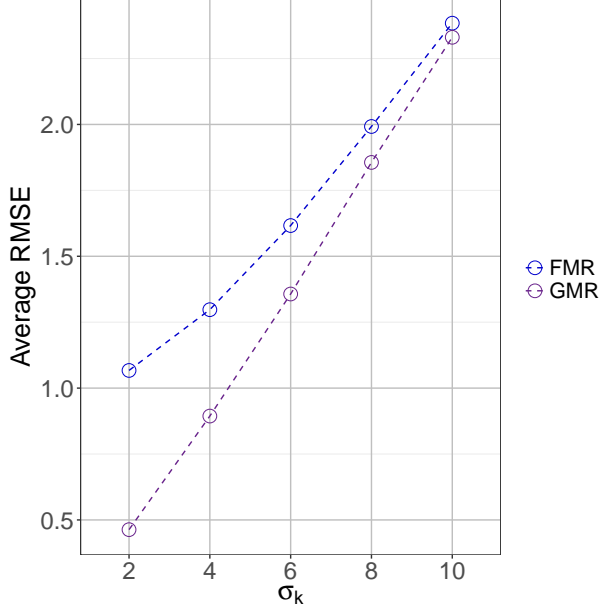


Figure 8: MAP prediction accuracy of the GMR (purple) versus the regular FMR (blue).

average RMSE; the prediction setup is as described earlier. Although both algorithms are very close in prediction performance, at higher uncertainties ($\sigma_k > 5$ and $\delta_\beta = 4$), GMR outperforms MMCL++ in predicting new observations.

4 Case Study: Dealership Performance Assessment

In this section, we present the results from applying the proposed GMR to a real-world problem in the retail industry. We show how to use GMR to provide guidelines and recommendations for improving the performance of retail stores, and in particular, the automotive dealerships. We apply the GMR to fit mixture of regression models to a dealership dataset in order to cluster the stores while accounting for the similarities in store performance dynamics.

4.1 Dealership Dataset

For reasons of confidentiality, we are not able to reveal full details about the dataset. The dataset made available to us consists of several thousands (3,074) dealerships, with consecutive monthly financial data (observations) for each dealer spanning five years (60

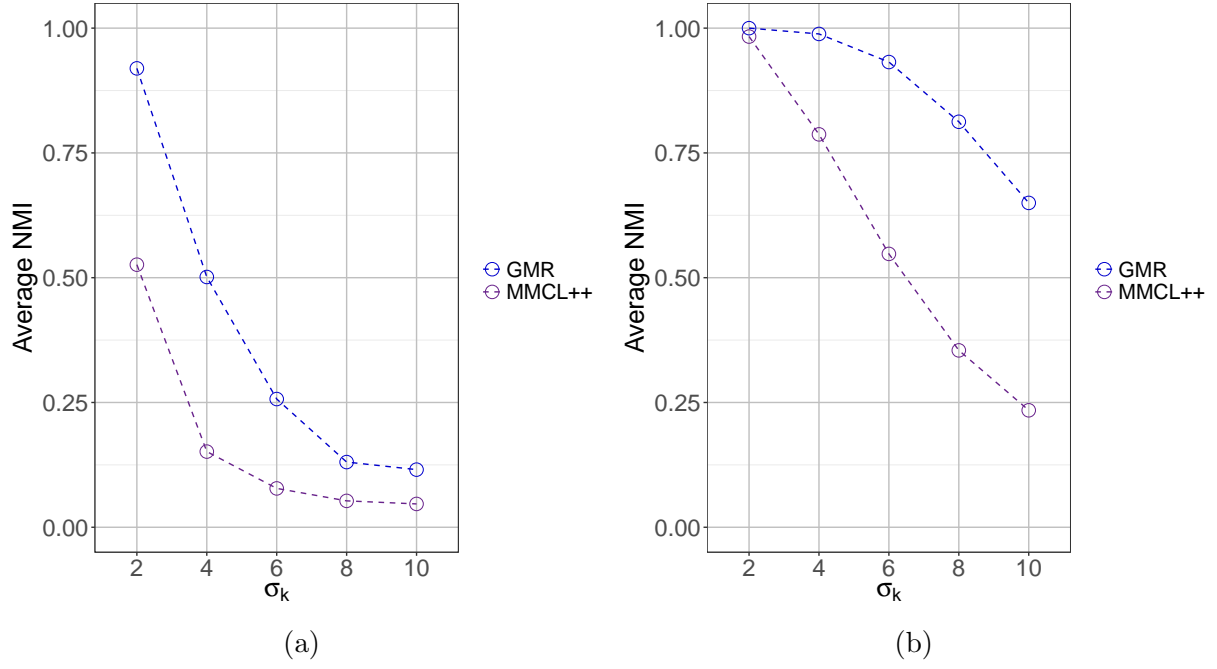


Figure 9: Label recovery of the MMCL++ versus the GMR: Average NMIs for (a) $\delta_\beta = 4$, (b) $\delta_\beta = 12$. In all cases $n = 100$.

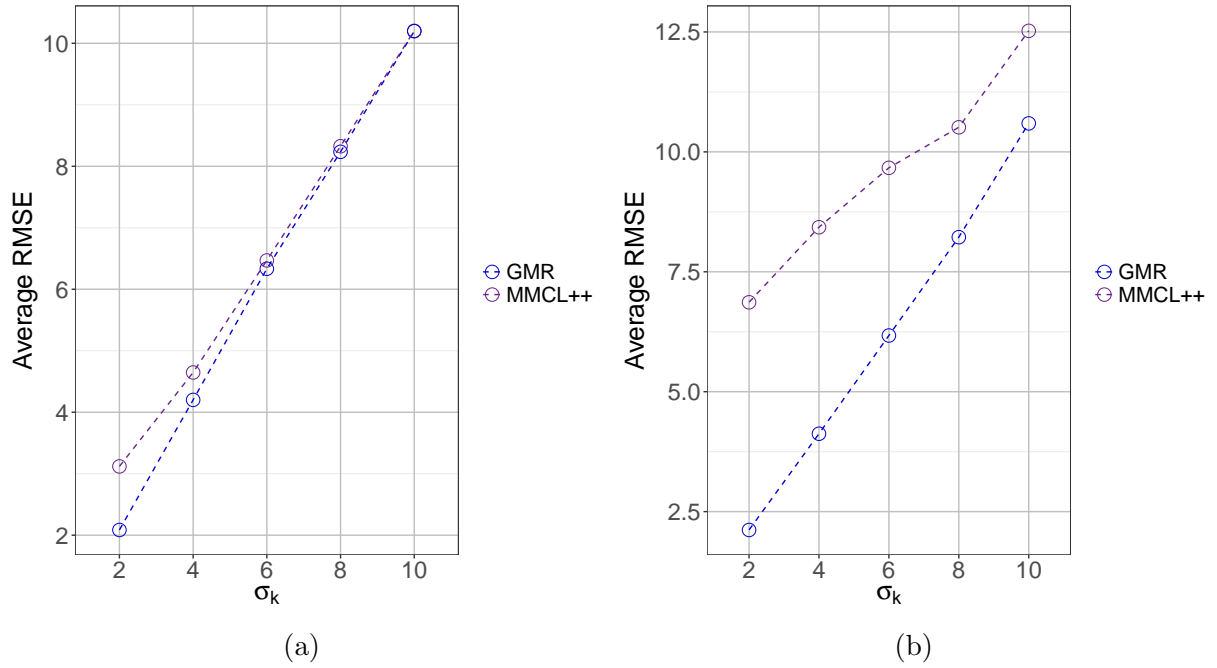


Figure 10: Comparing the prediction power of MMCL++ and GMR: Average RMSE value ($n = 100$) for (a) $\delta_\beta = 4$, (b) $\delta_\beta = 12$

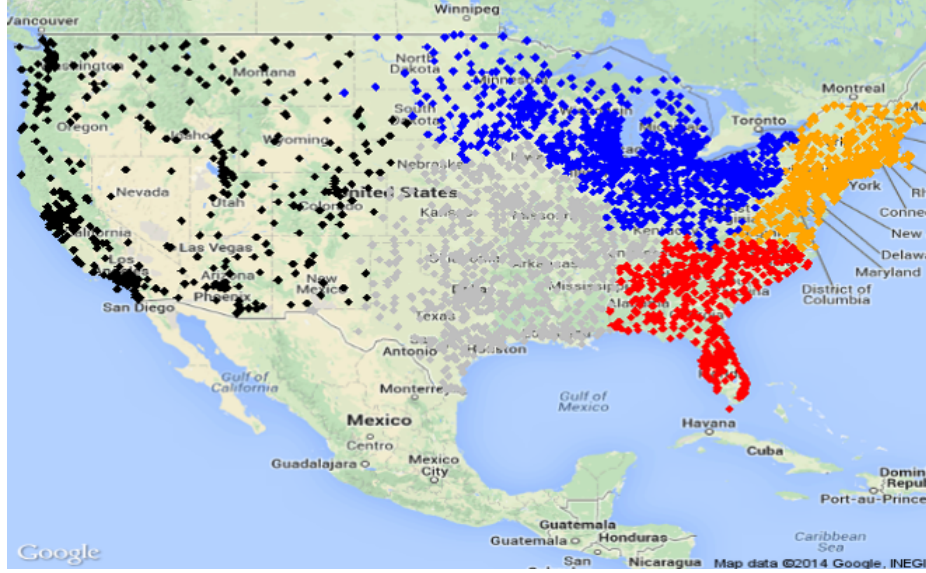


Figure 11: Network of OEM dealerships in the continental U.S. grouped by regions: Northeast (golden), Southeast (red), Great Lakes (blue), Central (gray), and West (black)

observations per dealer). Figure 11 shows the dealer network across the United States. It shows how the dealers are distributed and grouped into five regions: Northeast (yellow), Southeast (red), Great Lakes (blue), Central (gray), and West (black). There were 281 Key Performance Indicators (KPIs) in the monthly financial documents deemed important by the domain experts. We treat these KPIs as independent variables and standardize them to have zero mean and unit standard deviation.

To prepare the data for the application of the GMR, the observations for all the dealers are first aggregated to construct the design matrix $X \in \mathbb{R}^{(3074 \times 60) \times 281}$. Since the data for each dealership is generated for each month, we checked for trends and seasonality for each dealer and found no evidence that there exists trends or seasonality between the consecutive months. The reason is that the KPIs are constructed in a way that the trend and seasonality are absorbed by a special normalization procedure. The observations for each dealer are treated as a single group and assigned a unique group ID. That is, the number of groups in our setup is the same as the number of dealers.

4.2 Dealership Performance Prediction

In this section, we provide the results from applying the proposed GMR approach for modeling the productivity of automotive dealerships across the U.S. for a particular Original Equipment Manufacturer (OEM). We compare the results of the GMR with those of the MMCL++ (Almohri et al., 2018). Because of the large size of the dataset and specially the large number of predictors, Least Absolute Shrinkage and Selection Operator (LASSO) technique (Tibshirani, 1996) is used for regression modeling of both the sales as well as the profitability when MMCL++ is applied. To apply the GMR, the number of clusters (K) has to be identified in advance. As demonstrated by the simulations in Section 3.1, GMR can properly select the true K by cross-validation. The same process is applied to the dealership dataset to find the best K .

4.2.1 Results

Figure 12 summarizes the results. The plots report the prediction R^2 (i.e., over the test portion of the dataset) for both the performance metrics (“profitability”, the concern of the dealership, and the “sales effectiveness”, the OEM’s main objective). We are displaying the results from running the GMR and MMCL++ for $K \in \{2, \dots, 10\}$. The case $K = 1$ (the horizontal dashed line in the figure) corresponds to fitting a single linear regression model to the entire training dataset.

As the results suggest, GMR has improved the accuracy for predicting both the profitability and sales effectiveness metrics. It was able to achieve a R^2 value of 0.6 using $K = 9$ and $K = 10$, whereas the model with a single component has R^2 of 0.51, a 9% improvement. The highest R^2 that MMCL++ was able to achieve for profitability is 0.52 (with $K = 4$ and $K = 6$). In the case of sales effectiveness, the single component model is able to produce a R^2 value of 0.12. However, GMR was able to improve this value to 0.17 (41% improvement) with $K = 9$. MMCL++ also produced the same result with $K = 5$. This result also suggests that there is heterogeneity among the dealers and by clustering them, one can improve the analysis and generate better recommendations to dealers for improving their performance.

Reviewing Figure 12, we conclude that if GMR is used, we should ideally cluster the

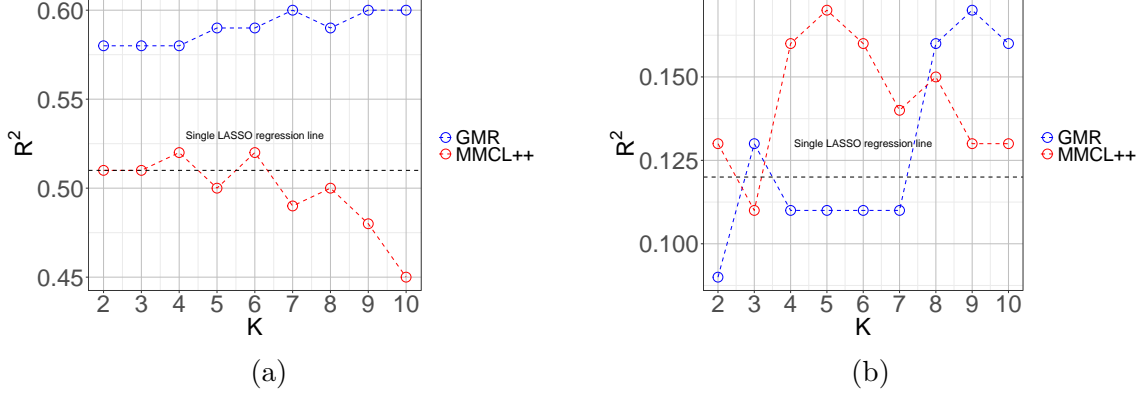


Figure 12: Results from applying MMCL++, and GMR to the dealership dataset with two dependent variables: (a) profitability and (b) sales effectiveness. The horizontal black dashed line is the R^2 for a single LASSO model.

dealers into 9 groups where the models show the highest R^2 for both the profitability and the sales effectiveness. In the case of modeling with MMCL++, it is best to partition the dealers into 4 clusters.

It should be mentioned that in large datasets such as our dealership problem, the MMCL++ approach is computationally more expensive. This is in general true when the number of groups is large, because the algorithm has to extract, model, and evaluate the results of all the groups in every iteration. The issue is even more problematic when employing cross-validation to find the best tuning parameters (such as K) as well as establishing the initial groups. This is not the case for GMR, for it had no problem handling and producing the results for such a large dataset in seconds on a regular laptop.

4.2.2 Assessing the Clusters

To evaluate the clusters resulting from GMR, we applied the GMR to a region within the U.S. as requested by the domain experts. The number of clusters K is set to 2. The following plots are produced to visually evaluate the effectiveness of the formed clusters. Figure 13 shows the average values for the two most important KPIs (i.e., those with the highest regression coefficients), plotted for the two clusters: cluster 1 in red and cluster 2 in blue. The plots only includes the last 36 months of the data for a better visualization.

As shown in Figure 13, the average value of KPI #1 in Figure 13a is clearly different

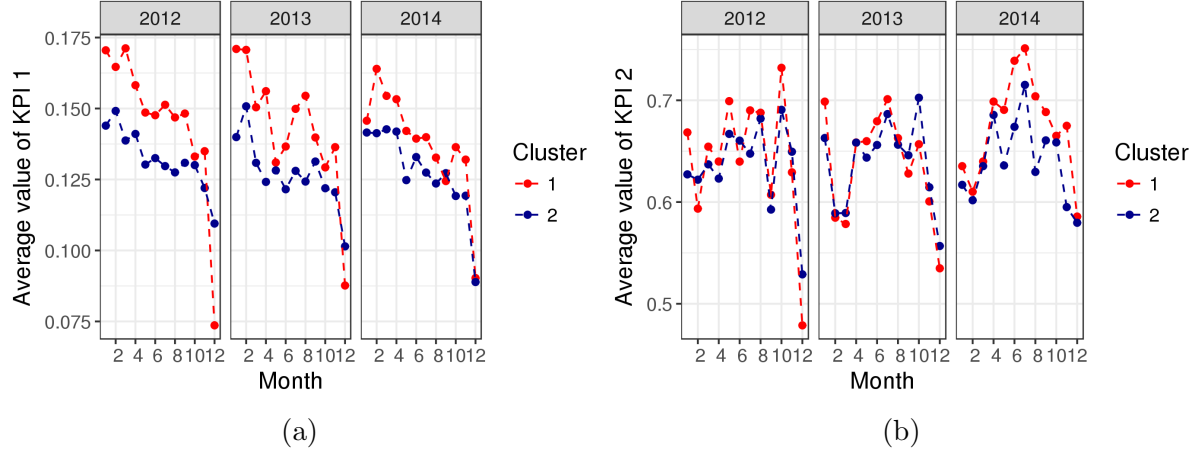


Figure 13: Assessing the clusters formed by GMR in the KPI space. The average value for each month and year is displayed for Cluster 1 (red) and Cluster 2 (blue) (a) KPI #1 (b) KPI #2

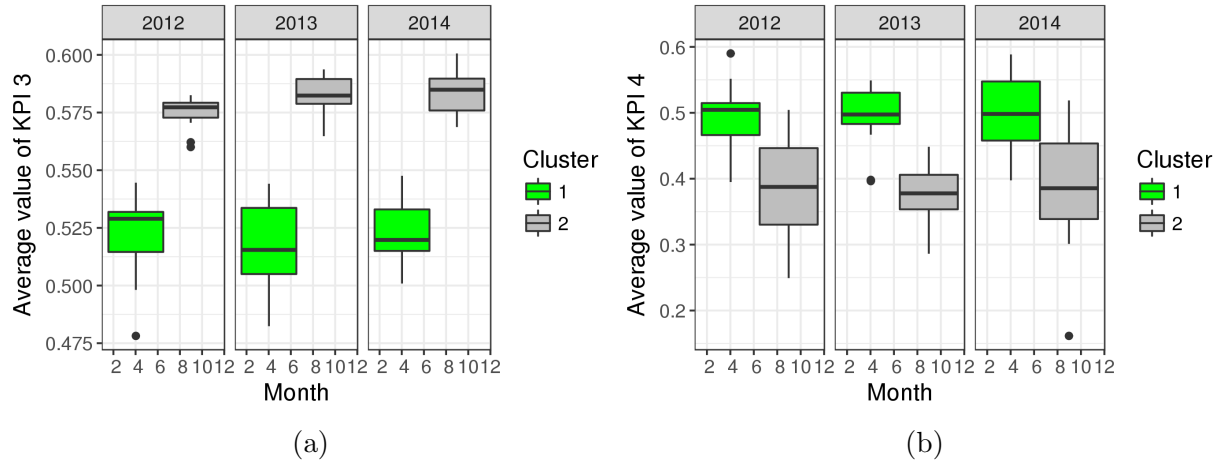


Figure 14: Box Plot for assessing the clusters formed by GMR in the KPI space. Values for each month and year is displayed for Cluster 1 (green) and Cluster 2 (gray) (a) KPI #3 (b) KPI #4

between the two clusters and cluster 2 (red) tends to contain the dealers that have a smaller value in that particular KPI. In the case of KPI #2 in Figure 13b, there are some months that the two clusters have overlapped, but the two clusters still seem to be different. Figure 14 shows box plots for two other important KPIs, separated by the clusters. This Figure also proves the effectiveness of GMR in forming clusters with members with different KPI ranges.

5 Conclusion

In this study, we introduced a solution to the mixture of regressions problem with observation group structure, which we term Grouped Mixture of Regressions (GMR). We derived the EM updates for this model providing a very fast algorithm for fitting the model. In addition, by deriving the predictive density we showed how the knowledge of the group membership of the new observations improves the prediction in the GMR versus the usual mixture of regressions.

Monte Carlo simulation experiments confirm the robustness of the algorithm and improved predictive performance. Using cross-validation, GMR successfully selected the optimal number of components which, in general, is a challenging task for any clustering technique. In addition, we performed an empirical study to compare the GMR with another recent heuristic algorithm proposed by [Almohri et al. \(2018\)](#), namely **MMCL++**. The experiments suggest that GMR outperforms **MMCL++** in both the recovery of the true clusters as well as the prediction accuracy. We also demonstrated the effectiveness of the algorithm in a real-world problem (predicting automotive dealership performance) and confirmed the superior performance of the GMR relative to the **MMCL++** in this real-world setting.

There are several avenues for potential future research. The current version of the GMR assumes that the covariates (features) are deterministic. This assumption can be relaxed by considering the model that treats the covariates as random. It is also possible to extend the approach to Generalized Linear Models (GLM) setting to expand the potential range of applications.

References

- Almohri, H., R. B. Chinnam, and M. Colosimo (2018). *Working Paper, Wayne State University*.
- Andrews, R. L. and I. S. Currim (2003). Retention of latent segments in regression-based marketing models. *International Journal of Research in Marketing* 20(4), 315–321.
- Bar-Shalom, Y. (1978). Tracking methods in a multitarget environment. *Automatic Control, IEEE Transactions on* 23(4), 618–626.

- Basu, S. (2009). *Constrained clustering: Advances in algorithms, theory, and applications*. Boca Raton: CRC Press.
- Bierbrauer, M., S. Trück, and R. Weron (2004). Modeling electricity prices with regime switching models. In *Computational Science-ICCS 2004*, pp. 859–867. Springer.
- Celeux, G. and J. Diebolt (1985). The SEM algorithm: A probabilistic teacher algorithm derived from the EM algorithm for the mixture problem. *Computational statistics quarterly* 2(1), 73–82.
- Celeux, G. and G. Govaert (1992). A classification em algorithm for clustering and two stochastic versions. *Computational statistics & Data analysis* 14(3), 315–332.
- De Veaux, R. D. (1989). Mixtures of linear regressions. *Computational Statistics & Data Analysis* 8(3), 227–245.
- Dempster, A. P., N. M. Laird, and D. B. Rubin (1977). Maximum likelihood from incomplete data via the EM algorithm. *Journal of the royal statistical society. Series B (methodological)*, 1–38.
- Faria, S. and G. Soromenho (2010). Fitting mixtures of linear regressions. *Journal of Statistical Computation and Simulation* 80(2), 201–225.
- Goutte, C., L. K. Hansen, M. G. Liptrot, and E. Rostrup (2001). Feature-space clustering for fMRI meta-analysis. *Human brain mapping* 13(3), 165–183.
- Goutte, C., P. Toft, E. Rostrup, F. Å. Nielsen, and L. K. Hansen (1999). On clustering fMRI time series. *NeuroImage* 9(3), 298–310.
- Honarkhah, M. and J. Caers (2010). Stochastic simulation of patterns using distance-based pattern modeling. *Mathematical Geosciences* 42(5), 487–517.
- Lemke, W. (2006). *Term structure modeling and estimation in a state space framework*, Volume 565. Springer Science & Business Media.
- Lletí, R., M. C. Ortiz, L. A. Sarabia, and M. S. Sánchez (2004). Selecting variables for k-means cluster analysis by using a genetic algorithm that optimises the silhouettes. *Analytica Chimica Acta* 515(1), 87–100.

- Newcomb, S. (1886). A generalized theory of the combination of observations so as to obtain the best result. *American Journal of Mathematics*, 343–366.
- Pearson, K. (1894). Contributions to the mathematical theory of evolution. *Philosophical Transactions of the Royal Society of London. A* 185, 71–110.
- Pelleg, D., A. W. Moore, et al. (2000). X-means: Extending k-means with efficient estimation of the number of clusters. In *ICML*, Volume 1, pp. 727–734.
- Permuter, H., J. Francos, et al. (2003). Gaussian mixture models of texture and colour for image database retrieval. In *Acoustics, Speech, and Signal Processing, 2003. Proceedings.(ICASSP'03). 2003 IEEE International Conference on*, Volume 3, pp. III–569. IEEE.
- Quandt, R. E. and J. B. Ramsey (1978). Estimating mixtures of normal distributions and switching regressions. *Journal of the American statistical Association* 73(364), 730–738.
- Reynolds, D., R. C. Rose, et al. (1995). Robust text-independent speaker identification using gaussian mixture speaker models. *Speech and Audio Processing, IEEE Transactions on* 3(1), 72–83.
- Stylianou, Y., Y. Pantazis, F. Calderero, P. Larroy, F. Severin, S. Schimke, R. Bonal, F. Matta, and A. Valsamakis (2005). GMM-based multimodal biometric verification. In *eINTERFACE 2005 The summer Workshop on Multimodal Interfaces July 18th–August 12th, Faculté Polytechnique de Mons, Belgium*.
- Tibshirani, R. (1996). Regression shrinkage and selection via the LASSO. *Journal of the Royal Statistical Society. Series B (Methodological)*, 267–288.
- Tuma, M. and R. Decker (2013). Finite mixture models in market segmentation: A review and suggestions for best practices. *Electronic Journal of Business Research Methods* 11(1).
- Wagstaff, K., C. Cardie, S. Rogers, and S. Schrödl (2001). Constrained k-means clustering with background knowledge. In *Proceedings of the Eighteenth International Conference on Machine Learning*, ICML '01, San Francisco, CA, USA, pp. 577–584. Morgan Kaufmann Publishers Inc.

A Appendix: EM Updates for Algorithm 1

Expanding the expected log-likelihood (7) using the definition of $\gamma_{rk}(\theta)$ in (3), we have

$$F(\theta; \hat{\theta}) = E_{z \sim \tau(\hat{\theta})}[\ell(\theta; z)] = \sum_{k=1}^K \tau_{+k}(\hat{\theta}) \log \pi_k + \sum_{r=1}^R \sum_{k=1}^K \sum_{i=1}^{n_r} \tau_{rk}(\hat{\theta}) \log \phi_{\sigma_k}(y_{ri} - \beta_k^T x_{ri}). \quad (9)$$

where $\phi_{\sigma}(t) := (2\pi\sigma^2)^{-1/2} \exp(-\frac{1}{2}t^2/\sigma^2)$ is the density of $N(0, \sigma^2)$.

We would like to maximize (9) over θ . Recall that $\beta_k, x_{ri} \in \mathbb{R}^p$ where p is the number of features. We will use $\dot{=}_{\pi}$ for example, when the two sides are equal up to additive constants, as functions of π . Fixing everything and maximizing over $\pi = (\pi_1, \dots, \pi_k)$, we are maximizing $\pi \mapsto \sum_k \tau_{+k}(\hat{\theta}) \log \pi_k$ over probability vector π . This is the MLE in the multinomial family and the solution is $\pi_k \propto_k \tau_{+k}$, that is

$$\pi_k = \frac{\tau_{+k}}{\sum_{k'} \tau_{+k'}} = \frac{\tau_{+k}}{R} \quad (10)$$

where we used $\sum_{k'} \tau_{+k'} = \sum_{k'} \sum_r \tau_{rk'} = \sum_r \sum_{k'} \tau_{rk'} = \sum_r 1 = R$, since for fixed r , τ_{rk} sums to 1 over k .

To maximize over β , we again fix everything else. Since $\log \phi_{\sigma}(t) \dot{=}_t -\frac{1}{2}(\log \sigma^2 + t^2/\sigma^2)$, we are maximizing

$$\begin{aligned} F(\theta; \hat{\theta}) &\dot{=}_{\beta} - \sum_r \sum_k \sum_i^{n_r} \tau_{rk}(\hat{\theta}) \frac{1}{2\sigma_k^2} (y_{ri} - \beta_k^T x_{ri})^2 \\ &\dot{=}_{\beta} - \sum_r \sum_k \sum_i^{n_r} \tau_{rk}(\hat{\theta}) \frac{1}{2\sigma_k^2} [(\beta_k^T x_{ri})^2 - 2y_{ri}\beta_k^T x_{ri}] \end{aligned} \quad (11)$$

ignoring the constant terms generated by y_{ri}^2 .

Note that $(\beta_k^T x_{ri})^2 = (\beta_k^T x_{ri})(x_{ri}^T \beta_k) = \beta_k^T (x_{ri} x_{ri}^T) \beta_k$. Similarly, $y_{ri} \beta_k^T x_{ri} = \beta_k^T (y_{ri} x_{ri})$. Let us define

$$\hat{\Sigma}_r := \frac{1}{n_r} \sum_{i=1}^{n_r} x_{ri} x_{ri}^T, \quad \hat{\rho}_r := \frac{1}{n_r} \sum_{i=1}^{n_r} y_{ri} x_{ri} \quad (12)$$

Summing over i first in (11), we get

$$\begin{aligned} F(\theta; \hat{\theta}) &\doteq_{\beta} - \sum_r \sum_k \frac{\tau_{rk}}{2\sigma_k^2} n_r [\beta_k^T \hat{\Sigma}_r \beta_k - 2\beta_k^T \hat{\rho}_r] \\ &= - \sum_k \frac{1}{2\sigma_k^2} \sum_r \tau_{rk} n_r [\beta_k^T \hat{\Sigma}_r \beta_k - 2\beta_k^T \hat{\rho}_r] \end{aligned} \quad (13)$$

Let us define $w_{rk} := n_r \tau_{rk}$ and $\check{w}_{rk} := w_{rk}/w_{+k}$ where $w_{+k} = \sum_r n_r \tau_{rk}$, and let

$$\tilde{\Sigma}_k := \sum_{r=1}^R \check{w}_{rk} \hat{\Sigma}_r, \quad \tilde{\rho}_k := \sum_{r=1}^R \check{w}_{rk} \hat{\rho}_r. \quad (14)$$

Dividing and multiplying by w_{+k} and summing over r in (13), we get

$$F(\theta; \hat{\theta}) \doteq_{\beta} - \sum_k \frac{w_{+k}}{2\sigma_k^2} [\beta_k^T \tilde{\Sigma}_k \beta_k - 2\beta_k^T \tilde{\rho}_k]. \quad (15)$$

The problem is separable in k , and the minimizer over β_k is $\beta_k = \tilde{\Sigma}_k^{-1} \tilde{\rho}_k$.

To optimize over $\alpha_k := \sigma_k^2$, let us fix everything else. We have

$$F(\theta; \hat{\theta}) \doteq_{\alpha} - \frac{1}{2} \sum_k \left[\sum_r \sum_i^{n_r} \tau_{rk} \log \alpha_k + \sum_r \sum_i^{n_r} \tau_{rk} \frac{(y_{ri} - \beta_k^T x_{ri})^2}{\alpha_k} \right]. \quad (16)$$

The first term in brackets is $(\sum_r n_r \tau_{rk}) \log \alpha_k = w_{+k} \log \alpha_k$. Defining

$$E_{rk} := E_{rk}(\beta) := \frac{1}{n_r} \sum_i^{n_r} (y_{ri} - \beta_k^T x_{ri})^2, \quad \bar{E}_k := \bar{E}_k(\beta) := \sum_r \check{w}_{rk} E_{rk}. \quad (17)$$

we see that the second term in brackets in (16) is just $w_{+k} \bar{E}_k$. We have

$$F(\theta; \hat{\theta}) \doteq_{\alpha} - \frac{1}{2} \sum_k w_{+k} \left[\log \alpha_k + \frac{\bar{E}_k}{\alpha_k} \right] \quad (18)$$

This problem is separable in α_k and the solution is $\alpha_k = \bar{E}_k$. Putting the pieces together, we obtain the Algorithm 1.

B Appendix: Details for β -error Calculation

Let $\hat{C}_k \subset [R]$ be the k th estimated cluster (containing indices of the groups estimated to be in cluster k) and $\hat{z}_r \in \{0, 1\}^K$ the estimated membership vector for group r , so that $\hat{z}_{rk} = 1\{r \in \hat{C}_k\}$. Similarly, let $C_k \subset [R]$ be the true cluster k and z_r the true label vector for group r , so that $z_{rk} = 1\{z_r \in C_k\}$. The normalized confusion matrix $F = (F_{k\ell}) \in [0, 1]^{K \times K}$ between the two sets of labels is given by $F_{k\ell} = \frac{1}{R} \sum_{r=1}^R z_{rk} \hat{z}_{r\ell} = \frac{1}{R} \sum_{r=1}^R 1\{r \in C_k, r \in \hat{C}_\ell\}$. Then, the following desired result is obtained:

$$\begin{aligned}
 \frac{1}{R} \sum_{r=1}^R \|\hat{\beta}^{(r)} - \beta^{(r)}\|^2 &= \frac{1}{R} \sum_{r=1}^R \left[\sum_{k,\ell=1}^K 1\{r \in C_k, r \in \hat{C}_\ell\} \right] \|\hat{\beta}^{(r)} - \beta^{(r)}\|^2 \\
 &= \sum_{k,\ell=1}^K \frac{1}{R} \sum_{r=1}^R 1\{r \in C_k, r \in \hat{C}_\ell\} \|\hat{\beta}^{(r)} - \beta^{(r)}\|^2 \\
 &= \sum_{k,\ell=1}^K \frac{1}{R} \sum_{r=1}^R 1\{r \in C_k, r \in \hat{C}_\ell\} \|\hat{\beta}_\ell - \beta_k\|^2 \\
 &= \sum_{k,\ell=1}^K \|\hat{\beta}_\ell - \beta_k\|^2 \frac{1}{R} \sum_{r=1}^R 1\{r \in C_k, r \in \hat{C}_\ell\} \\
 &= \sum_{k,r} D_{kr} F_{kr} = \text{tr}(D^T F)
 \end{aligned}$$

C Appendix: Experiment & Results Details

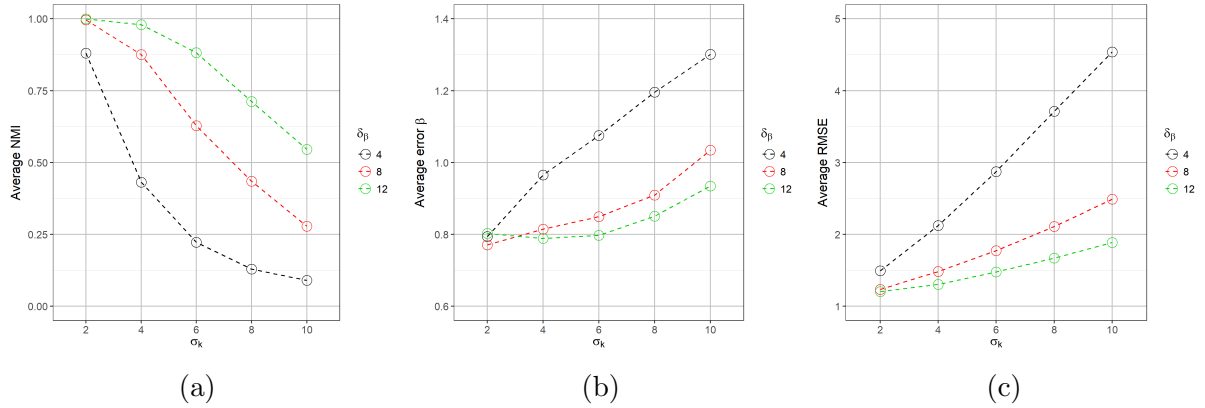


Figure 15: The effect of δ_β and σ_k for the case $n = 100, K = 2, p = 2$; each colored line in a plot represents different value of δ_β , X axis shows different values of σ_k , and y axis shows: (a) average NMI, (b) average β estimation error, (c) average RMSE for prediction

Figure 16 illustrates the impact of K and p on β estimation error. By comparing the plots in

Table 2: NMI Performance

		$\delta_\beta = 4$					$\delta_\beta = 7$					$\delta_\beta = 11$				
N	σ_k	2	4	6	8	10	2	4	6	8	10	2	4	6	8	10
$K=2; d=2$	100	0.88	0.43	0.22	0.13	0.09	0.99	0.87	0.62	0.43	0.27	0.99	0.98	0.88	0.71	0.54
	200	0.98	0.71	0.40	0.25	0.15	0.99	0.98	0.88	0.68	0.54	1	0.99	0.97	0.92	0.82
	400	0.99	0.91	0.68	0.46	0.32	1	0.99	0.98	0.90	0.81	1	1	0.99	0.98	0.96
	800	1	0.99	0.98	0.90	0.75	1	1	1	0.99	0.99	1	1	1	1	1
$K=2; d=4$	100	0.93	0.49	0.21	0.13	0.09	0.99	0.93	0.73	0.48	0.32	0.99	0.99	0.93	0.8	0.64
	200	0.99	0.82	0.45	0.26	0.16	1	0.99	0.94	0.80	0.62	1	0.99	0.99	0.97	0.91
	400	1	0.97	0.79	0.54	0.35	1	1	0.99	0.97	0.89	1	1	1	0.99	0.99
	800	1	0.99	0.96	0.84	0.64	1	1	1	0.99	0.98	1	1	1	1	0.99
$K=4; d=4$	100	0.80	0.34	0.20	0.15	0.12	0.97	0.80	0.52	0.34	0.25	0.98	0.94	0.81	0.62	0.45
	200	0.95	0.61	0.33	0.21	0.17	0.97	0.95	0.81	0.61	0.44	0.97	0.97	0.95	0.86	0.75
	400	0.96	0.86	0.58	0.38	0.27	0.96	0.96	0.94	0.86	0.72	0.96	0.96	0.96	0.95	0.92
	800	0.95	0.95	0.84	0.64	0.47	0.95	0.95	0.96	0.95	0.92	0.96	0.95	0.96	0.96	0.96

Figure 16, it is hard to find a consistent pattern for the behavior of the β estimation error with respect to p and K . What could be noticed is that in the case where $K = 2$ and $p = 2$, the error is less sensitive to increasing the noise (σ_k). However, the error stays higher when the noise is smaller (between 2-6). In the case of $\sigma_k = 10$, the highest error belongs to the case $K = 4, p = 4$.

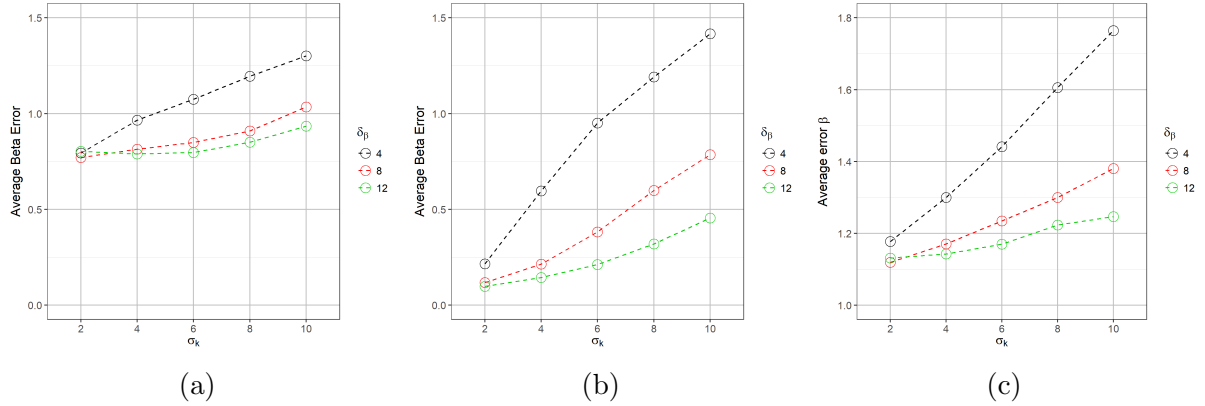


Figure 16: The impact of K and p on β estimation error for the case $n = 100$; each colored line in a plot represents different value of δ_β , X axis shows different values of σ_k , and y axis is average NMI for: (a) $K = 2, p = 2$, (b) $K = 2, p = 4$, (c) $K = 4, p = 4$

Table 3: β Error

		β -distance = 4					β -distance = 7					β -distance = 11				
N	σ_k	2	4	6	8	10	2	4	6	8	10	2	4	6	8	10
$K=2; d=2$	100	0.79	0.96	1.07	1.19	1.42	0.77	0.81	0.85	0.90	1.03	0.8	0.78	0.79	0.85	0.93
	200	0.76	0.81	0.97	1.06	1.15	0.78	0.81	0.79	0.87	0.90	0.79	0.76	0.78	0.81	0.81
	400	0.79	0.76	0.85	0.96	1.02	0.79	0.79	0.8	0.82	0.85	0.78	0.79	0.76	0.81	0.79
	800	0.07	0.1	0.14	0.21	0.31	0.06	0.07	0.08	0.1	0.12	0.06	0.06	0.07	0.08	0.09
$K=2; d=4$	100	0.21	0.59	0.95	1.19	1.41	0.11	0.59	0.38	0.59	0.78	0.09	0.14	0.21	0.32	0.45
	200	0.14	0.32	0.63	0.88	1.06	0.09	0.15	0.21	0.32	0.47	0.08	0.11	0.14	0.18	0.25
	400	0.11	0.19	0.35	0.55	0.76	0.08	0.10	0.14	0.19	0.26	0.07	0.09	0.11	0.13	0.16
	800	0.09	1.40	0.20	0.31	0.46	0.07	0.09	0.11	0.13	0.17	0.06	0.07	0.09	0.10	0.12
$K=4; d=4$	100	1.17	1.3	1.44	1.60	1.76	1.12	1.17	1.23	1.3	1.38	1.13	1.14	1.41	1.62	1.83
	200	1.14	1.23	1.31	1.40	1.51	1.14	1.15	1.17	1.20	1.26	1.13	1.12	1.15	1.16	1.19
	400	1.14	1.13	1.21	1.29	1.36	1.13	1.13	1.16	1.16	1.19	1.13	1.14	1.13	1.14	1.15
	800	1.13	1.14	1.16	1.21	1.25	1.13	1.13	1.14	1.14	1.14	1.14	1.13	1.13	1.14	1.14

Table 4: RMSE Performance

		β -distance = 4					β -distance = 7					β -distance = 11				
N	σ_k	2	4	6	8	10	2	4	6	8	10	2	4	6	8	10
$K=2; d=2$	100	1.49	2.12	2.87	3.71	4.54	1.23	1.48	1.77	2.10	2.49	1.2	1.30	1.47	1.67	1.88
	200	1.23	2.11	2.87	3.69	4.51	1.23	1.47	1.76	2.10	2.49	1.20	1.32	1.46	1.66	1.88
	400	1.46	2.11	2.88	3.68	4.52	1.25	1.48	1.78	2.13	2.48	1.23	1.32	1.46	1.66	1.89
	800	1.39	2.06	2.83	3.6	4.49	1.18	1.4	1.7	2.06	2.44	1.13	1.26	1.4	1.6	1.833
$K=2; d=4$	100	1.45	2.10	2.86	3.69	4.53	1.23	1.45	1.75	2.11	2.50	1.18	1.30	1.44	1.65	1.86
	200	1.45	2.10	2.87	3.68	4.51	1.23	1.45	1.75	2.10	2.48	1.19	1.30	1.45	1.64	1.86
	400	0.14	2.10	2.86	3.67	4.51	1.24	1.45	1.75	2.10	2.47	1.19	1.30	1.45	1.64	1.86
	800	1.44	2.09	2.86	3.67	4.50	1.23	1.45	1.74	2.09	2.46	1.19	1.29	1.45	1.65	1.86
$K=4; d=4$	100	1.41	2.07	2.85	3.67	4.50	1.18	1.41	1.72	2.07	2.45	1.14	1.25	1.41	1.62	1.83
	200	1.41	2.06	2.84	3.66	4.49	1.19	1.40	1.72	2.06	2.45	1.15	1.26	1.41	1.61	1.82
	400	1.41	2.07	2.84	3.66	4.50	1.19	1.41	1.72	2.06	2.44	1.14	1.25	1.41	1.60	1.83
	800	1.41	2.06	2.84	3.65	4.49	1.19	1.41	1.72	2.07	2.44	1.14	1.25	1.41	1.60	1.82

Table 5: Number of Iterations

		β -distance = 4					β -distance = 7					β -distance = 11				
N	σ_k	2	4	6	8	10	2	4	6	8	10	2	4	6	8	10
$K=2; d=2$	100	14.1	53.7	84.2	100.2	109.0	4.9	14.3	32.9	53.7	71.3	3.8	7.5	13.6	27.2	40.1
	200	6.3	27.6	60.6	82.4	101.3	3.3	6.4	14.4	29.3	44.7	3.1	3.8	6.6	11.5	19.6
	400	3.6	12.3	33.2	55.4	74.1	2.9	3.6	6.4	12.9	20.4	2.8	3.0	3.5	5.6	8.3
	800	2.7	3.4	6.8	13.9	24.7	2.5	2.8	3	3.4	4.7	2.4	2.6	2.8	2.9	3.1
$K=2; d=4$	100	11.4	42.8	65.1	72.4	73.6	4.2	12.1	25.2	43.2	55.2	3.6	5.8	12.0	19.6	30.8
	200	4.8	20.6	45.8	65.4	73.4	3.2	4.8	11.2	20.5	32.8	3.1	3.4	4.7	8.2	13.7
	400	3.2	8.8	23.3	42.5	57.5	2.9	3.2	4.7	8.6	15.7	2.8	3.0	3.2	3.8	5.7
	800	2.8	4.0	9.5	19.7	34.2	2.5	2.8	3.1	3.8	6.1	2.4	2.6	2.8	3.1	3.3
$K=4; d=4$	100	41.1	114.0	149.7	163.2	171.1	13.0	40.5	81.1	113.4	134.1	8.5	20.1	39.3	67.9	94.1
	200	18.6	74.7	121.8	149.1	162.5	7.7	18.3	42.7	72.8	103.0	9.15	10.7	18.5	33.2	52.3
	400	11.6	36.5	81.5	117.1	142.7	11.3	12.3	20.2	36.2	59.8	11.0	11.8	12.8	17.1	25.4
	800	12.7	18.1	40.5	72.8	104.6	13.0	13.2	12.0	17.8	27.7	10.1	12.6	12.7	12.5	14.0